Size Structures Sensory Hierarchy in Ocean Life

Erik A. Martens[1,2,3,*], Navish Wadhwa[1,4,*],
Nis S. Jacobsen[1,2], Christian Lindemann[1,2],
Ken H. Andersen[1,2], and André Visser[1,2]

May 4, 2015

[1]Centre for Ocean Life
[2]National Institute of Aquatic Resources, Technical University of Denmark, Charlottenlund Slot, Jægersborg Alle, DK-2920 Charlottenlund, Denmark
[3]Department of Biomedical Sciences, Copenhagen University, Blegdamsvej 3, 2200 Copenhagen, Denmark
[4]Department of Physics, Technical University of Denmark, DK-2800 Kgs. Lyngby, Denmark

[*]These authors contributed equally to this study

Corresponding authors:
Erik A. Martens: erik.martens@sund.ku.dk
Navish Wadhwa: nawa@fysik.dtu.dk

Abstract

Life in the ocean is shaped by the trade-off between a need to encounter other organisms for feeding or mating, and to avoid encounters with predators. Avoiding or achieving encounters necessitates an efficient means of collecting the maximum possible information from the surroundings through the use of remote sensing. In this study, we explore how sensing mode and range depend on body size. We reveal a hierarchy of sensing modes determined by body size. With increasing body size, a larger battery of modes become available (chemosensing, mechanosensing, vision, hearing, and echolocation) as well as a longer sensing range. This size-dependent hierarchy and the transitions between primary sensory modes are explained on the grounds of limiting factors set by physiology and the physical laws governing signal generation, transmission and reception. We characterize the governing mechanisms and theoretically predict the body size limits for various sensory modes, which align very well with size ranges found in literature. The treatise of all ocean life, from unicellular organisms to whales, demonstrates how body size determines available sensing modes, and thereby acts as a major structuring factor of aquatic life.

keywords: ocean life, sensing modes, body size, sensing range, fluid physics, traits

1 Introduction

The marine pelagic environment is sparsely populated. To survive, organisms of all kinds, from bacteria to whales, must search and extract nutrition from a volume of

water millions of times their own body volume per day [46]. Finding mates takes even more effort [47, 45]. While searching is a challenge in itself, there is also the constant risk of predation. For these reasons, there is a strong evolutionary drive for organisms to continuously and efficiently gather as much information as is feasible on the proximity of prey, mates and predators. Here, we examine the means by which this information is gathered by marine pelagic organisms, that is, their sensory ability. In particular, we wish to understand the relationships between scale (the size of the organism) and the usability of the various types of senses (e.g., chemical, hydromechanical, visual, acoustic).

Indeed, size is a key parameter to characterize biological processes in marine environments [27, 51, 28, 85, 4, 46, 44]. A cursory examination (Figure 1) indicates that there is at least some size dependent organization as to which sensory modes organisms use in the marine pelagic environment. For instance, the very smallest organisms (e.g. bacteria) generally have only the ability to detect chemical signals, while for slightly larger animals (e.g. copepods), hydromechanical sensing of fluid deformation becomes an important sensory mode. For larger organisms, vision (e.g. crustaceans and fish), hearing (e.g. fish) and echolocation (e.g. toothed whales) become increasingly essential sensory modes. How can we understand this general pattern on the grounds of physiological and physical scaling rules? Our aim here is to determine the body size limits of different sensing modes based on physical grounds, and to explain how the sensory hierarchy is structured by size.

2 Sensing as a physical process

Our goal is to understand how size determines the sensory modes available to an organism. To this end we establish scaling relationships for the working of various senses with organism size. We restrict ourselves to those sensory modes that are the primary means of remotely detecting the presence of other organisms: chemosensing of compounds, mechanosensing of hydromechanical perturbations provoked by moving animals, image vision in sufficiently lit areas, hearing of acoustically transmitted sound waves in water, and their generation for echolocation. Prey acquisition, predator avoidance, and mating involve an organism and a target; thus, we refer to the *organism* of size L and the *target* of size L_t. The two lengths are related via the size preference $p = L_\mathrm{t}/L$ (p can be related to fundamental tasks: $p = 0.1$ for predation, $p = 1$ for mating, $p = 10$ for predator avoidance). Clearly, other modes such as electroreception [15] or magnetoception [38] play important roles in supplementing the above mentioned modes, and animals may switch between sensing modes in dependence of their proximity to the target; here, however, we restrict ourselves to the aforementioned senses and consider them as the predominant primary sensory modes.

It is possible to decompose the above senses into three fundamental sub-processes: ***Generation***. How are sensory signals generated? Animals emit signals by creating fluid disturbances, creating sounds or reflecting ambient light. Features of the target such as its size, L_t, affect the signal, for example, a large body reflects more light than a small one. Other senses require an action from the target, such as sound or a hydromechanical disturbance, whereas light and echolocation do not. Echolocation in

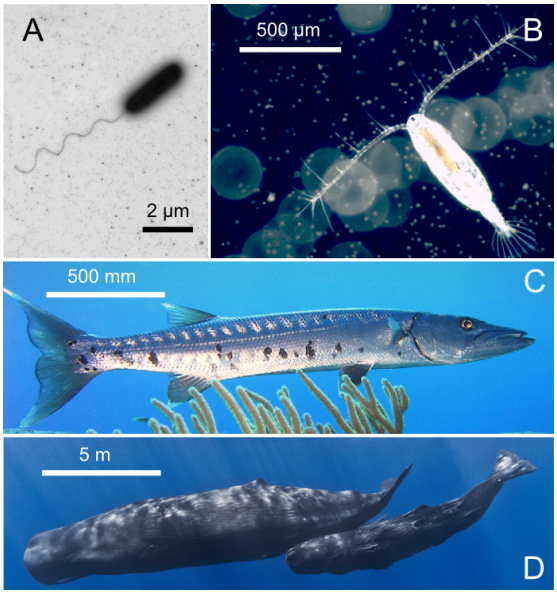

Figure 1: Organisms with different modes of perceiving their environment: (**A**) Bacteria (e.g. *Vibrio alginolyticus*) use chemosensing, and move up or down the gradients of chemicals (image courtesy Kwangmin Son and Roman Stocker, MIT). (**B**) Copepods (e.g. *Acartia Tonsa*) use hydromechanical signals to detect predators and prey in the vicinity (image courtesy of Thomas Kiørboe, DTU). (**C**) Fish (e.g. great barracuda *Sphyraena barracuda*) are often visual predators. (**D**) Toothed whales (e.g. *Physeter macrocephalus*) use echolocation. Images of the great barracuda and the sperm whale are in public domain.

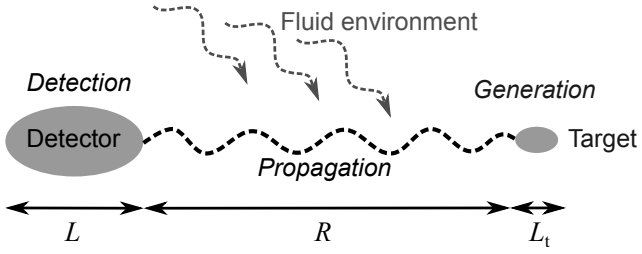

Figure 2: Schematic of the participants and the processes involved in sensing. The sizes of the target and the organism influence the generation and detection of the signal, while propagation through the fluid environment determines the sensing range.

particular can be termed an 'active sense', as the signal is generated by the organism. For active sensing, signal features such as intensity may be influenced by the organism size L.

Propagation. How effectively does a signal propagate through the fluid environment? The distance, over which a signal propagates before its strength drops below that of spurious noise, is sensitive to the fluid properties. For instance, the oceans are awash with traces of various compounds. Accordingly, detection of a specific compound requires concentrations higher than the background: the differentiability of the compound depends on its diffusivity, release rate, stability, and its dissimilarity to other competing background compounds. This distance sets a sensing range R.

Detection. What is an animal's ability to build a signal sensor given the physical constraints? This requires a cost-effective mechanism by which external information can be collected at a practical level of resolution. For example, the energetic costs of building a complex eye may far exceed an organism's available resources, or a large hydromechanical sensory array may give detailed information on approaching predators, but may compromise subsequent escape abilities.

Each of these sub-processes is constrained by the size of the animal. Thus the length scale imprints itself automatically on the remote detection both as a means to finding prey or mates, and for early warning of a predator attack. But limits of the usage of specific sensing modes are not necessarily clear-cut. For instance, in case of vision, the boundary between image forming eye (e.g. in fish) and non-image forming 'eye spots' which enable phototaxis (e.g. in copepods, protists) is not well defined, as the minimum resolution required to classify an eye as image forming has no definite value. Nevertheless, while the current investigation may not yield exact numerical values, it provides *characteristic* body size limits for the sensory modes and yields valuable understanding of the structure of sensing in marine life, based on first principles. In the following, we first analyse each of the senses mentioned above, followed by a synthesis to uncover the broad patterns and to compare with observations.

3 Chemosensing

The ability to detect chemical compounds is ubiquitous. All life forms have the ability to process chemical compounds and are equipped with the apparatus for chemosensing [1]. Chemotaxis and the use of chemosensing in remote detection can be divided into two modes: i) gradient climbing: moving along a gradient towards (or away from) a stationary target, and ii) detecting a trail laid out by a moving target [65, 5].

3.1 Size limits for chemosensing

Gradient climbing ability would be size independent were it not for two randomizing physical effects. At very small organism size, L, gradient climbing ability becomes impaired as the organism can no longer hold a steady course due to Brownian rotation [12]. Brownian rotation is caused by the impacts of the fluid molecules on the organism's body, which randomize its orientation, so that it cannot direct itself along a gradient using a biased random walk (Figure 3a). This becomes signifi-

cant for body sizes L less than the length scaling characteristic of Brownian motion, L_{Br} $(0.1 - 1\mu\mathrm{m})$ [64]. Using a similar argument, Dusenbery [22] has shown that the smallest body size at which an organism is capable of climbing chemical gradients using spatial or temporal comparisons of measured concentrations is around 0.6 μm. An upper limit for gradient climbing is imposed when turbulent dispersion disrupts the smoothness of the chemical gradient. This effect comes into play at L greater than the Batchelor scale $L_{\mathrm{B}} \approx (\nu D^2/\epsilon)^{1/4}$, where ν is the kinematic viscosity, D is the molecular diffusivity, and ϵ is the turbulent energy dissipation rate. L_{B} can be understood as the length scale at which diffusive time becomes comparable to the time over which energy is dissipated in smallest turbulent eddies (Figure 3b). The values for the turbulent energy dissipation rate ϵ in the ocean ranges between 10^{-8} and 10^{-3} m^2 s^{-3} [37, 79], L_{B} is between 5 μm and 100 μm in moderate turbulence (for a typical value of $D \sim 10^{-9}$ m ^{2} s $^{-1}$), but can become much larger in quiescent environments.

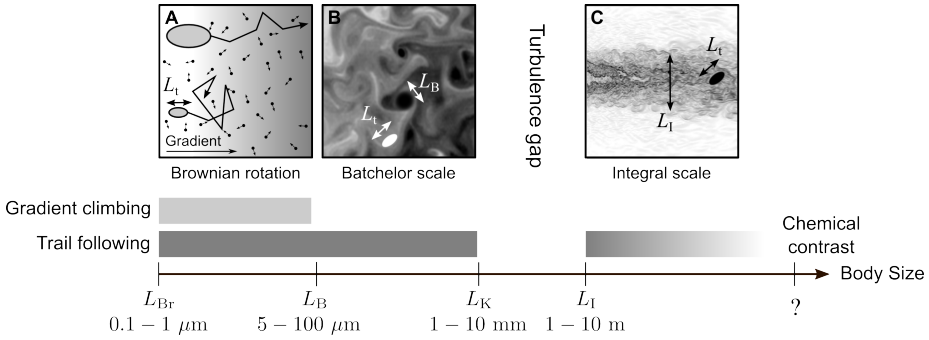

Figure 3: Length scales over which chemosensing can provide information by which an organism can locate a potential resource. A schematic illustration of Brownian rotation (A), Batchelor scale (B), and Integral scale (C) is included at the top.

For a moving target that releases a chemical trail, the physical constraints for the organism are similar to gradient climbing at small scales. Due to oceanic turbulence, a trail loses all directional information at the scale of the smallest turbulent eddies, defined as Kolmogorov scale $L_{\mathrm{K}} \approx (\nu^3/\epsilon)^{1/4}$, which is around a few millimetres in moderate turbulence. At size scales between L_{K} and the so called integral scale L_{I}, all directional information in the trail is lost due to the isotropy in turbulent flows, crippling chemotaxis for the organism if $L_{\mathrm{K}} < L < L_{\mathrm{I}}$. When $L > L_{\mathrm{I}}$, trail following becomes feasible again as the turbulent trail at this scale is anisotropic and contains the information regarding direction and size of the target (Figure 3c). Typical values for L_{I} in a stratified ocean are of the order 1 m or larger [88, 80].

Thus based on these arguments, it appears that chemosensing for gradient climbing may be a favourable sense for L between L_{Br} and L_{B}, and trail following to be favourable within two size ranges: a small scale range between up to L_{K}, and a large scale range, greater than L_{I}, where trail following again becomes feasible.

3.2 Sensing range for chemosensing

The size limits for functioning of chemosensing also apply to how far a target can be detected. For gradient climbing, when L is between L_{Br} and L_{B}, the maximal distance a chemical signal remains uninterrupted is limited to L_{B}; above this length the signal of the target is disrupted due to turbulent eddies. Another factor affecting the range for gradient climbing is the characteristic time scale of diffusion; for a typical chemical to diffuse over 1 cm it can take a duration of the order of days, making the signal irrelevant for many small organisms, either because they by that time have moved elsewhere, been preyed upon, have multiplied several times, or because the chemical compounds have degraded. Thus, gradient climbing due to its nature is relevant only up to small distances. Similarly, for trail following, sensing range is limited to L_{K}.

An absolute upper limit on sensing range is dictated by the requirement of sufficient chemical contrast. Chemosensing as a means of locating a target requires spatial variations in signal strength that can be detected and gradients therein tracked. However, chemical gradients tend to become eroded with time to some background level. The upper limit to the distance over which a trail can followed is not only related to the size and sensory ability of the organism, but also depends on the nature of the chemical substrate and its degradation in the environment due to microbial action or chemical reactions. Thus, while it is clear that an upper limit to trail following via chemosensing exists, it is not possible to quantify it.

4 Mechanosensing

Any movement made by an object in a fluid generates a hydromechanical disturbance that can potentially be detected with the appropriate sensory apparatus [81]. For many small organisms such as copepods, crustacean larvae, chaetognaths, and some protists [23, 14, 33, 48, 89], this is the dominant mechanism for interactions with their surroundings. The nature of a fluid disturbance is largely determined by the size and velocity of the object, and the Reynolds number (Re), which determines the relative importance of the inertial and viscous effects [72]. The Reynolds number for a moving target is defined as $\mathrm{Re} = L_{\mathrm{t}}U_{\mathrm{t}}/\nu$, where U_{t} is the swimming speed of the target, and ν is the kinematic viscosity [72]. For small Reynolds number, such as for most plankton, flow around an object is dominated by viscosity and is laminar [59]. For large Reynolds number, such as for large fish or marine mammals, inertia dominates, and the flow tends to be turbulent [10].

4.1 Propagation of fluid disturbances

For an target passively sinking at low Reynolds number, the velocity (u) induced in the surrounding fluid decays with distance r away from it as $u \sim r^{-1}$ [81]. The same is true for a feeding current of a stationary organism. For a self-propelled target, the induced velocity decays as $u \sim r^{-2}$ [81]. In recent studies, it was shown that for breast swimming plankton and impulsively jumping copepods at low to intermediate Reynolds number, u decays more rapidly as $u \sim r^{-3}$ and $u \sim r^{-4}$, respectively [36,

49]. At high Reynolds number, the fluid disturbance generated by an target is disrupted by ambient turbulence, if L_t is larger than L_K. A target swimming at high Reynolds number thus leaves a turbulent and noisy signal in its wake.

4.2 Detection

The setae arrayed along the first antenna of a copepod (Figure 4a) are a classic example of mechanosensors, which, when embedded in fluid moving at a velocity different from the copepod's body, bend and thus sense the fluid disturbances generated by other organisms, such by the prey nauplii (Figure 4b). It has been shown that setae are velocity sensors, and activate when the seta velocity exceeds a certain threshold [89]. This threshold defines the sensitivity s of the setae for fluid velocity detection [50], and is typically between 10 and 100 μm/s [81]. Similarly, in unicellular organisms such as ciliates and dinoflagellates, response typically occurs above a critical fluid deformation rate [63, 33], equivalent to a threshold velocity difference across the cell body. In general, mechanosensing requires a deformation on the organism's body, which can occur only if different parts of the organism experience different fluid velocities as a result of fluid deformation. Given a sensitivity s of a mechanosensor of size b, embedded in fluid with deformation rate Δ, the criterion for detection can be written as

$$\Delta \cdot b > s. \tag{1}$$

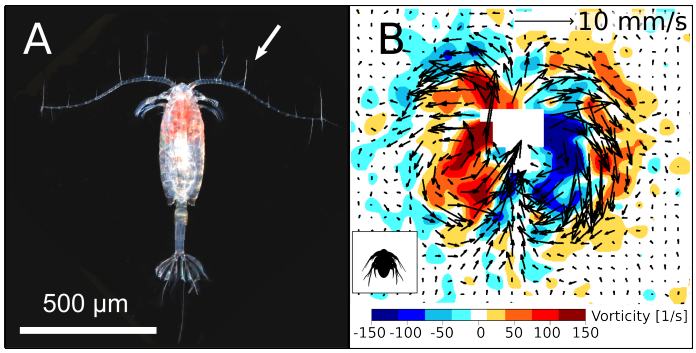

Figure 4: (**A**) Dorsal view of an adult *Acartia tonsa*, showing the antennules covered with mechanosensory setae, one of which is marked with an arrow (image courtesy of Erik Selander). (**B**) Flow disturbance created by a swimming *Acartia tonsa* nauplius, visualized in the form of velocity vectors and vorticity contours.

4.3 Sensing range for mechanosensing

To estimate the sensing range, we consider the case of a self propelling target. We assume that the sensing range R is larger than the sensor size b. For this situation, Visser [81] has shown that $R \approx (3U_t L_t^2 b/s)^{\frac{1}{3}}$. The swimming velocity of the target is related to its size by the empirical relation $U_t \sim c_1 L_t^{0.79}$ with $c_1 = 6.5\ \mathrm{m}^{0.21}/s$ [46]. If

we consider the case of prey detection, such that $p = 0.1$, and that the sensor is about a tenth of the body size, so that $b = L/10$, then we get

$$R \approx c_2 L^{1.26} \tag{2}$$

with $c_2 = 3.98\ \mathrm{m}^{-0.26}$.

From this estimate, a copepod of around 2 mm in length will have a prey sensing range of about 1.5 mm from the body. The coefficient for the scaling is determined by the exact morphology of the organism and the swimming characteristics of the target, but the range provides an order of magnitude estimate for how far a mechanosensitive organism can sense. An upper limit of R is set by the Kolmogorov scale L_K, at which, the range is comparable to the smallest eddies caused by oceanic turbulence, thus preventing mechanosensing from being useful to detect targets further than a few millimeters.

4.4 Size limits for mechanosensing

The smallest sized organism for which mechanosensing is still feasible is dictated by the inequality (1). For calculating the lower limit, we consider the case of a prey detecting a predator, such that the size ratio p = 10. For a target (predator) swimming with a velocity U_t, Δ scales in the limiting case as the ratio of U_t to its size L_t, such that $\Delta \sim U_\mathrm{t}/L_\mathrm{t}$. Using again the empirical scaling of $U_\mathrm{t} \sim c_2 L_\mathrm{t}^{0.79}$ [46], and further using the ratio $L = L_\mathrm{t}/10$, we can deduce that

$$\Delta \sim c_3 \cdot L^{-0.21}. \tag{3}$$

where $c_3 = 3.98\ \mathrm{m}^{0.21}\mathrm{s}^{-1}$.

To close the problem, we need the relationship between the size of sensor b and the organism size. We assume that the typical size of the sensory unit is about a tenth of the organism size, such that $b = L/10$. Then combining 1 and 3, substituting for b and using an intermediate value for s = 50 μm/s, we get a size limit of $L >$ 11 μm for a prey detecting a predator (p = 10). Thus, our simple argument suggests that the lower size limit for an organism to detect targets with mechanosensing is a few microns. Below this size, and given the sensitivity of mechanosensing apparatus, organisms are unable to detect the hydromechanical disturbances relevant to their size. The upper body size limit for mechanosensing, due to turbulent disturbance, is given by the Kolmogorov length scale $L_\mathrm{K} \sim 1$ cm.

5 Vision

Simple functions of vision include differentiating light from dark, for entrainment to a daily (circadian) rhythm [54] or for orientation [34], while more complex functions involve navigation, spatial orientation, visual communication [40] and pattern recognition for species identification and mating. An important function of vision is to detect prey and predators [2] from some distance, which requires a sufficiently high image resolution. In higher evolved organisms such as fish and mammals, this is achieved by

a complex optical system that collects light, forms an image through an arrangement of lenses, and converts it to neuro-electrical signals that are processed by the brain.

Eyes with resolution sufficient to discern prey have co-evolved in ten different forms, and 96% of animal species possess a complex optical system [56]. However, in general only two fundamental principles are used to build an eye: i) compound eyes, which comprise a number of individual lenses laid out on a convex surface, so that light is directly projected onto a spherically arranged array of photorecepting units (ommatidia), and ii) camera eyes with one concave photoreceptive surface where an image is projected onto the retina through an optical unit (pinhole or lens).

5.1 Light propagation in the marine environment

Given that a target is lit and visible, the reflected light must travel through seawater to reach the receiving organism. The intensity of light attenuates geometrically with distance r like r^{-2}. Further, attenuation of light is also due to scattering and absorption via the molecular structure of seawater or particulate matter (turbidity) [86]. There are different degrees of absorption depending on the wavelength of the light [19]. Generally, light intensity decreases like $e^{-\alpha r}$ where α is the called absorption coefficient [18].

5.2 Physiological limits to eye size

The resolution of the compound eye is limited by the size of individual ommatidia (photorecepting units in compound eyes). Physically, these cannot be reduced in size to achieve a resolution better than 1°. Thus, eyes of camera type, which we consider in the following, outperform compound eyes in terms of compactness [8, 25]. The function of a small eye is limited by two important constraints. First, a smaller eye is less sensitive as it captures less light. Secondly, a smaller eye can only achieve a smaller resolution: the photoreceptive units comprise the smallest components required to build an eye and are based on opsin molecules, which appear to be the universally represented light-capturing design in the animal world [56, 26].

Thus, the width of a photoreceptor (i.e., a foveal rod cell) $d_p \approx 1$ μm [16, 52] is an absolute limiting factor for any eye design (this argument neglects the space needed for maintenance of the retina and for the neural processing unit; both scale with image resolution). Therefore, n pixels amount to a retina diameter of $d = n^{1/2} d_p$. Considering a minimal required resolution for a usable image to be of 100^2 pixels, the corresponding retina would have a diameter $d \approx 0.1$ mm. Heuristic scaling laws regarding eye size are available for fish: $L_{\text{eye}} \approx c_4 \cdot L^{0.768}$ where $c_4 = 6 \cdot 10^{-3}$ m$^{0.232}$ [30]. It follows from this scaling that for the smallest eye with $L_{\text{eye}} \approx 0.1$ mm, the organism will have to be at least $L \approx 4$ mm long.

Arguments for an upper size limit for eyes are not evident on physical grounds. Larger eyes facilitate larger resolution and the largest known marine animals carry eyes (see Discussion). However, larger eyes comes with larger metabolic cost; further, the resulting higher resolution and sensitivity does not necessarily yield larger sensing range as it may be limited by turbidity, as we discuss next.

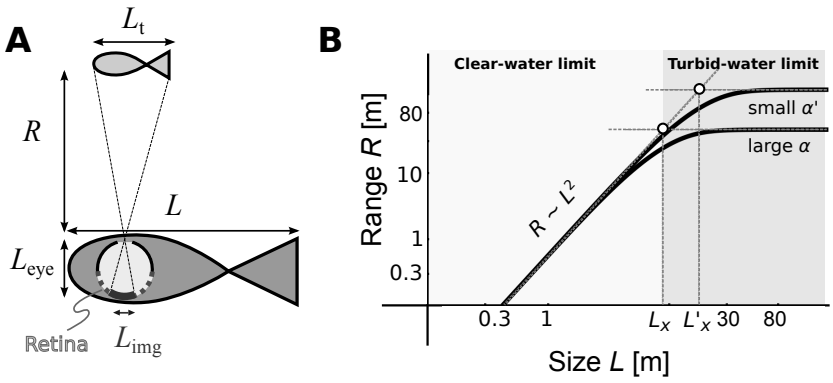

Figure 5: **A**: An organism of body size L, equipped with an eye of size $L_{\rm eye}$, may detect a target of size L_t at a distance R if the apparent contrast of the target is equal or larger than the threshold contrast of the organism's eye. The number of activated optical elements, n, is proportional to $L_{\rm img}^2$. **B**: Maximal visual sensing range scales with (minimal) body size L: like $R \sim L^2$ in the clear-water limit ($L \ll L_x$) and like $R \sim$ constant in the turbid-water limit ($L \gg L_x$). Parameters are $K = 0.025, C_0 = 0.3, C_{\rm th,min} = 0.05$ (adopted from [21]), $\alpha = 0.04$ m^{-1} [11] (α' = 0.01 m^{-1} for comparison) and $a = 1:30$.

5.3 Visual range

The visual range of an animal can be estimated by considering the properties of a (pinhole) camera eye, following an argument from a largely unrecognized work by [21]. In the following, we use Weber contrast, defined as $C = (I - I_b)/I_b$ where I and I_b are the intensities of the target and the background, respectively. The maximal distance R at which a predator can discern a prey of size $L_{\rm t}$ is determined by the following requirement: the apparent contrast $C_{\rm a}$ of the target at distance R must match the contrast threshold of the eye, $C_{\rm th}$. The inherent contrast of the target, C_0, declines with distance R yielding the apparent contrast of the target,

$$C_{\rm a} \quad = \quad C_0 \cdot e^{-\alpha R}, \tag{4}$$

see [18]. The contrast threshold is a declining function of the number of visual elements involved in perceiving the target:

$$C_{\rm th} = C_{\rm th,min}(z) + K_{\rm ph}/n. \tag{5}$$

This formula is partly based on Ricco's law [75] that expresses that the threshold contrast to is inversely proportional to the number of visual elements n, but does not account for the saturation of the contrast at a minimal value [68], and is therefore supplemented by adding the minimum contrast threshold $C_{\rm th,min}$ to represent this saturation limit. Note that the contrast threshold $C_{\rm th,min}$ varies in different environments and, in particular, depends on the available backlight at a given depth z. The projection of the visual image of the target on the organism's retina activates a number of visual elements n equal to the density of visual elements, σ, times the projected image

area. We can assume that R is large relative to the eye ball diameter $L_{\rm eye}$ so, employing the principle of similar triangles, the number of activated visual elements becomes $n = \sigma\,\pi/4\,L_{\rm img}^2 \approx \sigma L_{\rm eye}^2 L_o^2 R^{-2}$ (see Figure 5A). Noting the universal size of opsin molecule across species, we may assume that the density σ is independent of eye size. Introducing the ratio $a = L_{\rm eye}/L$ [30] and using $p = L_{\rm t}/L$, we get $n = \sigma a^2 p^2 L^4 R^{-2}$. The range R is determined by the condition that the apparent contrast must match the contrast threshold, $C_a \geq C_{\rm th}$:

$$C_0 e^{-\alpha R} \geq C_{\rm th,min}(z) + K R^2 L^{-4}, \tag{6}$$

where $K = K_{\rm ph}\sigma^{-1}a^{-2}p^{-2}$ is a constant characterizing the photoreceptor sensitivity ($K_{\rm ph}/\sigma$), eye size ratio, and size preference. Sample solutions for the condition $C_a = C_{\rm th}$, yielding the range R at a given size L, are shown in Figure 5B. Isolating R from (6) is impossible; however, asymptotic solutions are derivable for two limits:

(i) **"Clear-water limit"**: the visual range is limited by the resolution of the eye, i.e. we have that $\alpha \to 0$; thus, the maximal visual range is $R \sim [(C_0 - C_{\rm th,min})/K]^{1/2} L^2$.

(ii) **"Turbid-water limit"**: the visual range is limited by the sensitivity (the minimum contrast threshold) of a visual element, when $C_0 - C_{\rm th,min} \gg K R^2 L^{-4}$; thus, $R \sim (\ln C_0 - \ln C_{\rm th,min})/\alpha$. In this limit, R is independent of the predator size and is essentially limited by the minimum contrast threshold $C_{\rm th,min}$.

Generally, the visual range decreases if the light is limited, e.g. at large depth z, leading to a higher minimal threshold contrast $C_{\rm th,min}$ (cases (i) and (ii)); or if the turbidity is strong (larger α) (case (ii). The cross-over between the two limits occurs when $L \sim L_x \sim \alpha^{-1/2}$ (see Supplementary text). The visibility range in pure water for light of 550 nm is theoretically estimated at 74 m [76], and measurements in the open sea range from 44-80 m [17].

6 Hearing

Sound propagates through the ocean as pressure waves, resulting in the alternating compression and rarefaction of water in regions of high and low pressure, respectively. Any form of hearing must rely on detecting these pressure variations by converting them into vibrations of a body or membrane whose motion stimulates nerve cells. While hearing ability in many animals makes use of sound pressure waves directly, many fish and all marine mammals have in addition the ability to amplify the pressure waves [71, 18]. In fish, sound waves displace sensory hairs against the calcareous *otolith* (which remains stationary due to its higher density) and this relative motion is detected. In mammalian ears, sound pressure waves excite the tympanic membrane (ear drum), the motion of which is sensed by ciliary hair in the cochlea.

Most sounds relevant to ocean life, except echolocation, fall into the range of a few Hz up to a few kHz. Sounds generated by marine animals can originate from rapid movement or are produced for communication, the frequencies of which rarely exceed 1 kHz [42]. Communication by marine mammals usually consists of a burst of click (train) or of whistles (4-12 kHz), while the echolocating signals of foraging odontocete range between 20 and 200 kHz [43].

6.1 Underwater sound propagation

As sound waves travel through a medium, the sound intensity attenuates with distance from the target r, due to two processes: (i) geometric spreading (r^{-2} in open space), and (ii) absorption in water. The latter is frequency dependent (1 dB/km at 10 kHz, but only 10^{-4} dB/km at 100 Hz in seawater[1] and is smaller by a factor of nearly 100 in freshwater [18]). Sound is therefore only weakly attenuated in seawater, and it can potentially carry information over large distances.

6.2 Lower limit for sound detection

Effective detection of sound requires either an organism of significantly different density than that of water (e.g., the otolith), or an detector array (e.g., auricle and drum) larger than the wavelength of sound. In order to directly pick up sound waves, an otolith-like organelle has to move relative to the surrounding fluid, as explained above. Motions in small sound sensing organs (operating at low Re) are inherently more damped by viscosity than larger ones, further impairing the practicality of a small organism. With regards to wavelength of sound, the speed of sound in sea water is roughly 1530 m/s, so even a 10 kHz sound in seawater has a wavelength of around 15 cm. Thus a sensor array, congruent with the size of the organism, would have to be at least 15 cm in size. Thus hearing – both in terms of direct sensing of fluid motion or having a sensor array – is not practical for pelagic organisms smaller than a few centimetres.

Many pelagic fish have swim bladders which, through connections to the otolith containing cavity, act as amplifiers for sound [29]. Indeed, fish without swim bladders have poor hearing [29, 71]. Similarly, odontocetes use the fat-filled bones of their lower jaw as an amplifying cavity [43]. The swim bladders are air-filled structures, which amplify sound optimally when in natural resonance with the sound waves. Sounds of frequencies very different from the resonance frequency of the swim bladder do not amplify well, or if too different from the resonance frequency, may even be de-amplified [18]. Based on an assumption of a spherical air-filled swim bladder, the resonance frequency, f, can be approximated via [62, 3, 18]:

$$f = \frac{1}{2\pi r_{\mathrm{b}}}\sqrt{\frac{3\Gamma P}{\rho}} \tag{7}$$

where P is depth dependent hydrostatic pressure, r_{b} the radius of the swim bladder, ρ the density of sea water, and Γ the adiabatic exponent (~ 1.4 for air). The swim bladder radius is related to the fork-length in fish and measures around 5-10 % [13]. Using the upper limit of 10% (i.e. $r_{\mathrm{b}} = L/10$), for a conservative estimate, an organism's body size would need to be at least $L = 3$ cm at the sea surface, in order to amplify the high frequency end (1 kHz) of the ambient underwater sound spectrum, and $L = 11$ cm at a depth of 100 m (Figure 6). To hear the more typical lower frequencies, the organism's body size would have to be larger still. Thus, we approximate that the lower body size

[1]The decibel level is defined via $L_{\mathrm{dB}} = 10\log_{10}(I/I_0)$, where I is the sound intensity and I_0 is a reference frequency.

limit for detection of sound using swim bladders is $L \approx 1 \ldots 10$ cm, though note that this depends on the depth.

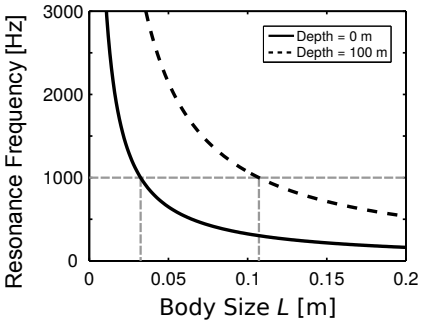

Figure 6: Relationship of body size and resonance frequency based on Equation 7 and using a swim bladder size $r_\mathrm{b} = L/10$ for an individual at the surface (solid curve) and at 100 m depth (dashed curve). The dashed (grey) horizontal line indicates 1 kHz, below which most sounds generated by marine live are found.

7 Echolocation

Echolocation is an active sensing mode, where the echolocating animal emits clicks in the ultrasonic range and interprets the environment based on the echo of these clicks. Echolocation is common in odontocetes (tooth whales) and is generally used for orientation, communication and prey detection. The generation of echolocating signals in tooth whales is associated with the nose passage leading up to the blowhole and takes place in the phonic lips. Taking into account anatomical structures, the frequency with the largest intensity produced in the nasal sac can be estimated with the resonance frequency of a Helmholtz oscillator [6]. The diffraction limit sets a resolution limit for the size of an target that can be resolved[18]

$$L_\mathrm{t} \quad < \quad \frac{\lambda}{2\pi}, \tag{8}$$

where $\lambda = c/f$ is the wave length of the click and $c = 1530$ m/s is the speed of sound in water. Given that dolphins and whales produce clicks which have peak energies at frequencies in the range of 20 to 200 kHz [43], the resulting resolution lies in the range from 1 to 8 mm. Taking a middle value (5 mm) as a typical smallest resolvable feature, and assuming that the target is an order of magnitude larger than the smallest resolvable feature, we get a minimal target size of 50 mm. Invoking the size preference ratio p and noting that echolocation is generally used for prey detection, such that p = 0.1, we get a lower organism body size for echolocation to be $L = 50/p$ = 500 mm. This simple argument suggests a lower size limit of echolocation to be a few hundred millimetres. The same argument also implies that objects smaller than about 1 mm do not scatter sound signals, allowing echolocation to effectively boost the sensing range

in turbid waters where vision is severely restricted. Taken together, echolocation is an effective way to sense up to large distances when vision is limited, but only for prey size (or swarms) larger than about 5-10 cm, i.e. fish and other larger organisms.

7.1 Sensing range

We estimate how the range of echolocation scales with body size L based on three assumptions:

1) the threshold sensitivity of the ear I_0 is independent of target size L_t. This approximation is supported by audiograms (behavioral and auditory brain stem responses) of odontocetes [67, 69, 70, 77, 20],

2) the emitted sound intensity that an animal produces scales with size: $I_e \propto L^{3\phi}$ where $3/4 < \phi < 1$,

3) the carrier frequency of the sonar signal depends on size L (see [35] and Supplementary Text).

The generated acoustic signal travels first through water, is then partially reflected by the target, and the remainder of the signal finally travels back to the receiving organism. Thus the originally emitted sound intensity, I_e, is reduced by two processes:

i) ***Reflection.*** The signal experiences a reduction upon reflection from the target where the reflected intensity is proportional to its area scaling like L_t^2.

ii) ***Attenuation.*** Sound intensity decreases with distance as r^{-2} due to geometric divergence. The intensity is further attenuated exponentially due to absorption processes in the seawater. Together, the signal intensity attenuates as $(2r)^{-2}e^{-2\mu r}$, where the factor 2 is due to the doubled travel distance.

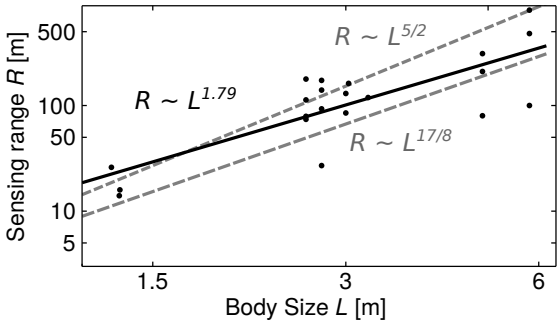

Figure 7: Comparison of the predicted echolocation sensing range (dashed grey) with data (black dots) [7, 9, 41, 66, 77], which scales like $R \approx 14.2\ \mathrm{m}^{-0.79} \cdot L^{1.79}$ (black line, least squares fit).

A detailed analysis shows that geometric attenuation strongly dominates over the absorption processes (see Supplementary text). Thus, we find that $I_r \sim I_e L_t^2 r^{-2} \sim L^{3\phi} L_t^2 r^{-2}$. The condition that the strength of the returned signal just balances the

threshold intensity for detection in the ear, $I_0 = I_r$, yields a sensing range $R \sim I_0^{-1} L^{3\phi/2} L_\mathrm{t}$. Introducing the size ratio $p = L_\mathrm{t}/L$, we arrive at

$$R \sim \frac{p}{I_0} L^\gamma, \tag{9}$$

where the exponent $\gamma = 1 + 3\phi/2$ lies in the range from 2.125 to 2.5. The exact value for the scaling factor depends on further unknown parameters, but it can be estimated using data describing the echolocation range of small marine mammals (see Fig. 7 and Supplementary text for details); the resulting scaling coefficient (including p/I_0) is 6.47 $\mathrm{m}^{-1.5}$ for $\gamma = 2.5$, and 9.79 $\mathrm{m}^{-1.25}$ for $\gamma = 2.125$, respectively. Taking into account the considerable scatter of data available for dolphins [7, 9, 41, 66, 77], yet we recognize that the prediction compares with the data reasonably well (Fig. 7).

8 Discussion

We have attempted to synthesize an understanding of how the physiology and the physical environment enables and constrains aquatic organisms' ability to gather information about their surroundings. By reducing the physical mechanisms involved in sensing to their simplest form, we have identified the most pressing constraints on the functioning of various senses. Our goal has been to theoretically explain the transitions in body size from one primary sense to another, as observed in nature. A comparison of the predicted size limits with those observed in nature underscores the usefulness of our analysis (Table 1, Figure 8). The predicted size ranges (shaded rectangles) correspond well with known minimal and maximal sizes of animals using a specific sense (dots), see Figure 8. The size range of a sense does not necessarily imply that an organism cannot detect the signal outside the limits at all, but rather that *beyond* these limits, the usefulness of the sense is compromised when compared with other senses.

Table 1: Lower and upper size (body length) limits for various senses. Predicted theoretical limits denote orders of magnitude.

	Observed limit				Theoretical limit	
	Lower [m]		Upper [m]		Lower [m]	Upper [m]
Chemosensing	$8 \cdot 10^{-7}$	[78]	30	[60]	10^{-7}	—
Mechanosensing	$3.5 \cdot 10^{-5}$	[58]	0.01	[53]	10^{-5}	10^{-2}
Vision	$1.5 \cdot 10^{-3}$	[73]	30	[60]	10^{-3}	—
Hearing	$9 \cdot 10^{-3}$	[87]	30	[60]	$3 \cdot 10^{-2}$	—
Echolocation	0.55	[39, 90]	18.6	[83]	0.5	—

We could not conceive any upper limits on physical grounds for chemosensing, hearing, and vision. Indeed, the largest known organism in the ocean, the blue whale (L = 30 m), is known to use all of these senses. Chemosensing is the only sense available to the smallest organisms, and its theoretical lower size limit ($L_\mathrm{Br} \sim 10^{-7} - 10^{-6}$ m) is consistent with the smallest known motile organisms (bacteria, L = 0.8 μm [22]). We hypothesize a "turbulence gap" in the usability of chemosensing as a dominant sensory mode, in the range of around $L_\mathrm{K} \sim 1$ cm and $L_\mathrm{I} \sim 1$ m. While we do not have strong evidence that such a gap exists, we note that the dominant group in that

size range, bony fish, rely on vision as a primary sensory mode [30]. Chemosensing for trail following is an important sensory mode for large fish [61] and sharks [31], which have sizes larger than L_{I}.

The lower theoretical limit for mechanosensing is found to be a few micrometers, in the realm of protists; to our knowledge, marine protists sized 7-10 μm are the smallest prey known to respond to ciliate predator attacks through remote mechanosensing [32]. The largest free-swimming copepods are almost a centimetre in size, close to the expected upper mechanosensing limit due to ambient turbulence ($L_{\mathrm{K}} \sim 10^{-2}$ m). Notably, this is also the size scale at which the smallest fully developed eyes are recorded.

The camera eye takes both records of smallest and largest eye (see Supplementary text): the smallest eyes (and body sizes) are found in the fish *Schindleria brevipinguis* [82] ($L \approx 7$ mm), and the pygmy squids ($L \approx 1.5$ mm) [73], which compares well with our predicted size limit. A curiosity are dinoflagellates in the genus *Erythropsidium* at a size of around 50 μm owning the smallest known eyes with a lens [74]; however, their image-forming capability seems dubious due to the lack of a complex brain for processing. The largest known eye belongs to the giant squid [55], featuring eye balls of up to 30 cm in diameter [57]. Smaller eyes are also found in the largest known species (whales), implying there is no upper body size limit for image-forming vision in marine animals.

For hearing, our arguments suggest a theoretical lower body size limit of a few centimetres. In reality, some fish are able to control the membrane elasticity of their swim bladder, enabling them to control the resonance frequency of swim bladders [24]. By using sub-optimal hearing of sound outside the resonance frequency, fish larvae of a few millimetres ($L \approx 9$ mm) have been found to react to sounds [87, 84]. Note that these fish inhabit shallower waters, where hearing is feasible at smaller sizes (Figure 6). For echolocation, the predicted lower limit (~ 0.5 m) has the same order of magnitude as the observed smallest size among echolocating marine mammals (Commerson's dolphin). The fact that the smallest feature resolvable with echolocation is a few millimetres in size, may also explain why baleen whales do not echolocate - their favoured prey (krill and smaller organisms) are too small to be detected.

We have estimated the range up to which a sense is capable of gathering information. To this end, we have investigated the limitations of the sensing range due to degradation of the signal via absorption, geometric spreading (divergence), or environmental noise. In the cases of chemosensing and mechanosensing, the chemical and mechanical signals are randomized beyond a certain distance (L_{B} and L_{K}, respectively) due to the ambient turbulence. On scales greater than the integral length scale L_I, the sensing range for chemosensing appears unlimited, as long as a sufficiently large chemical contrast is present. For mechanosensing we found that the maximal range scales as $R \sim L^{1.26}$ (Figure 8). When mechanosensing can no longer extend its range, vision becomes a viable solution. Vision is limited to a sensing range of $R \sim L^2$ but can never exceed the limit set by turbidity; however, even in clear waters, vision cannot exceed the range of approximately 80 m. Here, vision is complemented by the senses of hearing and echolocation mainly because sound with its larger wave lengths is capable of traveling large distances in sea water without attenuation. While we could not develop any such scaling for hearing, we could determine the sensing

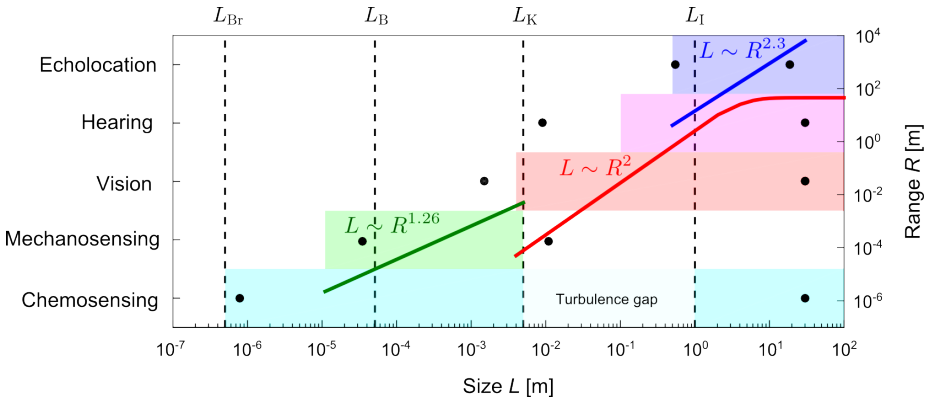

Figure 8: Upper and lower body size limits and range for different senses. The points denote the largest and smallest sizes known to employ a given sense, and shaded rectangles show the theoretical estimates of the size range in which a sense is expected to work. Green, red, and blue curves show the theoretical scaling of sensing range with size for mechanosensing, vision, and echolocation respectively.

range of echolocation with size, which approximately scales like $R \sim L^{2.3}$ and seems to be as large as kilometres for larger organisms, comparing well with the known range of marine mammals.

The question arises whether there is a general pattern underlying the size-structure of primary sensory modalities. For instance, can the transitions overs between primary senses be related to metabolic demand? Kleiber's law requires that an organism consumes energy at a rate proportional to $L^{9/4}$[51]; this demand must be matched with finding prey at a sufficient clearance rate [4]. The clearance rate is a function of swimming velocity $v \sim L^x$ and sensing range $R \sim L^y$ with positive exponents x, y, and thus the rate also increases with body size L . At the same time – given that investing into a specific sensory mode is linked to a size-dependent trade-off – one might suspect that the respective sense becomes too costly above a certain critical size L. An evolutionary pressure arises then to extend the sensing range by investing into other more energy efficient sensory strategies, thus causing the transition from one to the other primary sensory mode. However, rather than being governed by cost efficiency, it seems more plausible that the transitions between sensory modalities are simply set by the physical limitations of signal generation, transmission and reception that we discussed above. To exemplify, carrying larger eyes can in principle boost the eye's image resolution and sensitivity and thus extend the sensing range. But at the same time, having larger eyes also increases metabolic costs, which beyond a critical (eye) size becomes unsustainable. Instead, it seems that the increased performance of the eye is just rendered ineffective at larger sensing ranges due to the effects of turbidity, and so, the transition is explained as echolocation surpasses vision in achieving the required sensing range.

We have combined biological knowledge, physiology and physics to describe the abilities of the sensory modes in ocean life, from bacteria to whales. Our treatise

of oceanic life demonstrates how body size determines available sensing modes, and thereby acts as a major structuring factor of all aquatic life. In particular, we have examined how body size plays together with the physical constraints at different scales to shape the strategies available for organisms of different size. When interpreting the scalings and limits we propose in this work, it should be kept in mind that our purpose is to provide first order approximations for the size limits of a sense based on physical first principles. Future research is needed to evaluate properties of each of the senses in more detail and to gather more data to support some of the arguments presented here. We hope that our arguments may serve as a starting point for further explorations on sensory modalities and their hierarchical structures.

Acknowledgements

We would like to thank Thomas Kiørboe for helpful discussions and for comments on the manuscript. The Centre for Ocean Life is a VKR center of excellence supported by the Villum foundation (EAM, NW, CL, NSJ, KHA, AV). The work is part of the Dynamical Systems Interdisciplinary Network, University of Copenhagen (EAM). Partial financial support for CL was provided by EURO-BASIN (FP7, Ref. 264933).

References

[1] Julius Adler. Chemotaxis in bacteria. *Science*, 153(3737):708–716, 1966.

[2] Dag L. Aksnes and Jarl Giske. A theoretical model of aquatic visual feeding. *Ecological Modelling*, 67(2-4):233–250, June 1993.

[3] Scott Allen and David a Demer. Detection and characterization of yellowfin and bluefin tuna using passive-acoustical techniques. *Fisheries Research*, 63(3):393–403, September 2003.

[4] K H Andersen and J E Beyer. Asymptotic Size Determines Species Abundance in the Marine Size Spectrum. *Am. Naturalist*, 168(1), May 2006.

[5] John C. Andrews. Deformation of the active space in the low reynolds number feeding current of calanoid copepods. *Canadian Journal of Fisheries and Aquatic Sciences*, 40(8):1293–1302, 1983.

[6] JL Aroyan, MA McDonald, SC Webb, JA Hildebrand, D Clark, JT Laitman, and JS Reidenberg. Acoustic models of sound production and propagation. In *Hearing by whales and . . .* , number 2000. 2000.

[7] WWL Au and KJ Snyder. Long-range target detection in open waters by an echolocating Atlantic Bottlenose dolphin (Tursiopstruncatus). *The Journal of the Acoustical Society of . . .* , pages 1077–1084, 1980.

[8] HB Barlow. The size of ommatidia in apposition eyes. *Journal of Experimental Biology*, (May):667–674, 1952.

[9] Lance G Barrett-Lennard, John K Ford, and Kathy A Heise. The Mixed Blessing of Echolocation: Differences in Sonar Use by Fish-Eating and Mammal-Eating Killer Whales. *Animal Behaviour*, 51:553–565, 1996.

[10] George Keith Batchelor. *An introduction to fluid dynamics*. Cambridge University Press, Cambridge, UK, 1967.

[11] Aike Beckmann and Inga Hense. Beneath the surface: Characteristics of oceanic ecosystems under weak mixing conditions – A theoretical investigation. *Progress in Oceanography*, 75(4):771–796, December 2007.

[12] H. C. Berg. A physicist looks at bacterial chemotaxis. In *Cold Spring Harbor Symposia on Quantitative Biology*, volume 53, pages 1–9, 1988.

[13] JHS Blaxter. The swimbladder and hearing. *Hearing and sound communication in fishes*, 1981.

[14] HowardI. Browman, Jeannette Yen, DavidM. Fields, Jean-François St-Pierre, and AnneBerit Skiftesvik. Fine-scale observations of the predatory behaviour of the carnivorous copepod paraeuchaeta norvegica and the escape responses of their ichthyoplankton prey, atlantic cod (gadus morhua). *Marine Biology*, 158(12):2653–2660, 2011.

[15] Shaun P Collin and Darryl Whitehead. The functional roles of passive electroreception in non-electric shes. *Animal Biology*, 54(1):1–25, 2004.

[16] Christine A. Curcio, Kenneth R. Sloan, Robert E. Kalina, and Anita E. Hendrickson. Human photoreceptor topography. *The Journal of Comparative Neurology*, 292(4):497–523, 1990.

[17] R. J. DaviesColley and D. G. Smith. Optically pure waters in waikoropupu ('pupu') springs, nelson, new zealand. *New Zealand Journal of Marine and Freshwater Research*, 29(2):251–256, 1995.

[18] Mark W Denny. *Air and water: the biology and physics of life's media*. Princeton University Press, 1993.

[19] E. J. Denton. Light and vision at depths greater than 200 metres. In *Light and Life in the Sea*, chapter 8, pages 127–148. Cambridge University Press, Cambridge, UK, 1990.

[20] DOSITS.org. What sounds can animals hear? *Discovery of Sound in the Sea (dosits.org)*, 2014.

[21] R L Dunbrack and D M Ware. Energy constraints and reproductive trade-offs determining body size in fishes. In P. Calow, editor, *Evolutionary Physiological Ecology*, pages 191–218. 1987.

[22] David B. Dusenbery. Minimum size limit for useful locomotion by free-swimming microbes. *Proceedings of the National Academy of Sciences*, 94(20):10949–10954, 1997.

[23] David Feigenbaum and M. R. Reeve. Prey detection in the Chaetognatha: Responseto a vibrating probe and experimental determination of attack distance in large aquaria. *Limnology and Oceanography*, 22:1052–1058, 1977.

[24] C Feuillade and RW Nero. A viscous-elastic swimbladder model for describing enhanced-frequency resonance scattering from fish. *The Journal of the Acoustical Society of* . . . , (February 1997):3245–3255, 1998.

[25] R. P. Feynman. Color Vision. In Michael A. (Caltech) Gottlieb and Rudolf (Caltech) Pfeiffer, editors, *The Feynman lectures on physics*, chapter Chapter 35. California Institute of Technology, 2013.

[26] T.H. Goldsmith. Optimization, constraint, and history in the evolution of eyes. *Quarterly Review of Biology*, 65(3):281–322, 1990.

[27] J. B. S. Haldane. On being the right size. *Harper's Magazine*, 1926.

[28] Per Juel Hansen, Peter Koefoed, and Benni Winding Hansen. Zooplankton grazing and growth: Scaling within the 2-1000 μm body size range. 42(4):687–704, 1997.

[29] AD Hawkins. Underwater sound and fish behaviour. In *The behaviour of teleost fishes*, page 1986. 1986.

[30] Howard C Howland, Stacey Merola, and Jennifer R Basarab. The allometry and scaling of the size of vertebrate eyes. *Vision research*, 44(17):2043–65, January 2004.

[31] Robert E Hueter, David A Mann, Karen P Maruska, Joseph A Sisneros, and Leo S Demski. Sensory biology of elasmobranchs. *Biology of sharks and their relatives*, pages 325–368, 2004.

[32] Hans Henrik Jakobsen, LM Everett, and SL Strom. Hydromechanical signaling between the ciliate mesodinium pulex and motile protist prey. *Aquatic microbial ecology*, 44(2):197–206, 2006.

[33] HH Jakobsen. Escape response of planktonic protists to fluid mechanical signals. *Marine Ecology Progress Series*, 214:67–78, 2001.

[34] Gáspár Jékely, Julien Colombelli, Harald Hausen, Keren Guy, Ernst Stelzer, François Nédélec, and Detlev Arendt. Mechanism of phototaxis in marine zooplankton. *Nature*, 456(7220):395–9, November 2008.

[35] Frants H Jensen, Alice Rocco, Rubaiyat M Mansur, Brian D Smith, Vincent M Janik, and Peter T Madsen. Clicking in shallow rivers: short-range echolocation of irrawaddy and ganges river dolphins in a shallow, acoustically complex habitat. *PloS one*, 8(4):e59284, January 2013.

[36] Houshuo Jiang and Thomas Kiørboe. The fluid dynamics of swimming by jumping in copepods. *Journal of the Royal Society Interface*, 8:1090–1103, 2011.

[37] Javier Jiménez. Oceanic turbulence at millimeter scales. *Scientia Marina*, 61:47–56, 1997.

[38] Sönke Johnsen and Kenneth J Lohmann. The physics and neurobiology of magnetoreception. *Nature Reviews Neuroscience*, 6(9):703–712, 2005.

[39] BE Joseph, JE Antrim, and LH Cornell. Commerson's dolphin (Cephalorhynchus commersonii): a discussion of the first live birth within a marine zoological park. *Zoo biology*, 77:69–77, 1987.

[40] Maarten Kamermans and Craig Hawryshyn. Teleost polarization vision: how it might work and what it might be good for. *Philosophical transactions of the Royal Society of London. Series B, Biological sciences*, 366(1565):742–56, March 2011.

[41] R A Kastelein, W W Au, H T Rippe, and N M Schooneman. Target detection by an echolocating harbor porpoise (Phocoena phocoena). *The Journal of the Acoustical Society of America*, 105:2493–2498, 1999.

[42] a. O. Kasumyan. Sounds and sound production in fishes. *Journal of Ichthyology*, 48(11):981–1030, December 2008.

[43] DR Ketten. The marine mammal ear: specializations for aquatic audition and echolocation. *The evolutionary biology of hearing*, pages 717–750, 1992.

[44] R. J. Gonçalves M. Hartvig J. Heuschele S. Hylander N.S. Jacobsen C. Lindemann E.A. Martens A.B. Neuheimer K. Olsson A. Palacz F. Prowe J. Sainmont S.J. Traving A.W. Visser N. Wadhwa K.H. Andersen, T. Berge and T. Kiørboe. Characteristic sizes of life in the oceans, from bacteria to whales. *Annual Review of Marine Sciences*, (in press).

[45] Thomas Kiørboe. Mate finding, mating, and population dynamics in a planktonic copepod Oithona davisae: There are too few males. *Limnology and Oceanography*, 52:1511–1522, 2007.

[46] Thomas Kiørboe. How zooplankton feed: Mechanisms, traits and trade-offs. *Biological Reviews*, 86:311–339, 2011.

[47] Thomas Kiørboe and Espen Bagøien. Motility patterns and mate encounter rates in planktonic copepods. *Limnology and Oceanography*, 50:1999–2007, 2005.

[48] Thomas Kiørboe, Houshuo Jiang, and Sean P Colin. Danger of zooplankton feeding: the fluid signal generated by ambush-feeding copepods. *Proceedings of the Royal Society B: Biological Sciences*, 277:3229–3237, 2010.

[49] Thomas Kiørboe, Houshuo Jiang, Rodrigo Javier Gonçalves, Lasse Tor Nielsen, and Navish Wadhwa. Flow disturbances generated by feeding and swimming zooplankton. *Proceedings of the National Academy of Sciences*, 111(32):11738–11743, 2014.

[50] Thomas Kiørboe and Andre Visser. Predator and prey perception in copepods due to hydromechanical signals. *Marine Ecology-Progress Series*, 179:81–95, 1999.

[51] Max Kleiber. Body size and metabolism. *Hilgardia*, 6:315–351, 1932.

[52] Helga Kolb, Ralph Nelson, Eduardo Fernandez, and Bryan Jones. Part II: Anatomy and physiology of the retina: Photoreceptors. . In *WEBVISION: The organization of the Retina and Visual System*. 2014.

[53] K.N. Kosobokova, H.-J. Hirche, and R.R. Hopcroft. Reproductive biology of deep-water calanoid copepods from the arctic ocean. *Marine Biology*, 151(3):919–934, 2007.

[54] Georg Kreimer. The green algal eyespot apparatus: a primordial visual system and more? *Current genetics*, 55(1):19–43, February 2009.

[55] Tsunemi Kubodera and Kyoichi Mori. First-ever observations of a live giant squid in the wild. *Proceedings. Biological sciences / The Royal Society*, 272(1581):2583–6, December 2005.

[56] M F Land and R D Fernald. The evolution of eyes. *Annual review of neuroscience*, 15(1990):1–29, January 1992.

[57] M. F. Land and D. E. Nilsson. *Animal eyes*. Oxford University Press, 2002.

[58] Michael I. Latz, Michelle Bovard, Virginia VanDelinder, Enrico Segre, Jim Rohr, and Alex Groisman. Bioluminescent response of individual dinoflagellate cells to hydrodynamic stress measured with millisecond resolution in a microfluidic device. *Journal of Experimental Biology*, 211(17):2865–2875, 2008.

[59] Eric Lauga and Thomas R Powers. The hydrodynamics of swimming microorganisms. *Reports on Progress in Physics*, 72(9):096601, September 2009.

[60] C. Lockyer. Body weights of some species of large whales. *Journal du Conseil*, 36(3):259–273, 1976.

[61] Svein Løkkeborg. Feeding behaviour of cod,< i> Gadus morhua</i>: activity rhythm and chemically mediated food search. *Animal behaviour*, 56(2):371–378, 1998.

[62] RH Love. Resonant acoustic scattering by swimbladder-bearing fish. *The Journal of the Acoustical Society of America*, 64(May):571–580, 1978.

[63] Elisa M. Maldonado and Michael I. Latz. Shear-stress dependence of dinoflagellate bioluminescence. *The Biological Bulletin*, 212(3):242–249, 2007.

[64] James G Mitchell. The influence of cell size on marine bacterial motility and energetics. *Microbial ecology*, 22(1):227–238, 1991.

[65] Paul A. Moore, David M. Fields, and Jeannette Yen. Physical constraints of chemoreception in foraging copepods. *Limnology and Oceanography*, 44:166–177, 1999.

[66] A. Earl Murchison. *Animal Sonar Systems*. Springer US, Boston, MA, January 1980.

[67] Paul E. Nachtigall, T. Aran Mooney, Kristen a. Taylor, and Michelle M. L. Yuen. Hearing and Auditory Evoked Potential Methods Applied to Odontocete Cetaceans. *Aquatic Mammals*, 33(1):6–13, January 2007.

[68] D. Northmore, F. C. Volkmann, and D. Yager. Vision in fishes: colour and pattern. In D. I. Mostofsky, editor, *The Behavior of Fish and Other Aquatic Animals*, page 85. 1978.

[69] A F Pacini, P E Nachtigall, L N Kloepper, M Linnenschmidt, A Sogorb, and S Matias. Audiogram of a formerly stranded long-finned pilot whale (Globicephala melas) measured using auditory evoked potentials. *The Journal of experimental biology*, 213:3138–3143, 2010.

[70] Aude F Pacini, Paul E Nachtigall, Christopher T Quintos, T David Schofield, Dera a Look, Gregg a Levine, and Jason P Turner. Audiogram of a stranded Blainville's beaked whale (Mesoplodon densirostris) measured using auditory evoked potentials. *The Journal of experimental biology*, 214(Pt 14):2409–15, July 2011.

[71] Arthur N Popper and Richard R Fay. Rethinking sound detection by fishes. *Hearing research*, 273(1-2):25–36, March 2011.

[72] Constantine Pozrikidis. *Introduction to Theoretical and Computational Fluid Dynamics*. Oxford University Press, Oxford, UK, 2nd edition, 2011.

[73] A. Reid. Family Idiosepiidae. In P. Jereb and C. F. E. Roper, editors, *Cephalopods of the world, Vol. I*. 2005.

[74] I R Schwab. You are what you eat. *British Journal of Ophthalmology*, 88(9):1113–1113, September 2004.

[75] Steven Schwartz. *Visual perception: A Clinical Orientation*. McGraw-Hill Professional, 3rd edition, 2004.

[76] Raymond C Smith and Karen S Baker. Optical properties of the clearest natural waters (200-800nm). *Applied Optics*, 20(2):177–184, 1981.

[77] Jonas Teilmann, Lee A Miller, Tim Kirketerp, Ronald A Kastelein, Peter T Madsen, Bjarke K Nielsen, and Whitlow W L Au. Characteristics of echolocation signals used by a harbour porpoise (*Phocoena phocoena*) in a target detection experiment. *Aquatic Mammals*, 28:275–284, 2002.

[78] B Velimirov. Nanobacteria, Ultramicrobacteria and Starvation Forms: A Search for the Smallest Metabolizing Bacterium. *Microbes and Environments*, 16(2):67–77, 2001.

[79] A. W. Visser, H. Saito, E. Saiz, and T. Kiørboe. Observations of copepod feeding and vertical distribution under natural turbulent conditions in the north sea. *Marine Biology*, 138(5):1011–1019, 2001.

[80] Andre Visser. Small, wet & rational: Individual based zooplankton ecology, 1997.

[81] AW Visser. Hydromechanical signals in the plankton. *Marine Ecology Progress Series*, 222:1–24, 2001.

[82] W. Watson and H. J. jr. Walker. The world's smallest vertebrate, Schindleria brevipinguis, a new paedomorphic species in the family Schindleriidae (Perciformes: Gobioidei). *Records of the Astralian Museum*, 56:139–142, 2004.

[83] Stephanie L Watwood, Patrick J O Miller, Mark Johnson, Peter T Madsen, and Peter L Tyack. Deep-diving foraging behaviour of sperm whales (Physeter macrocephalus). *The Journal of animal ecology*, 75(3):814–25, 2006.

[84] J. F. Webb, R. M. Walsh, B. M. Casper, Mann D. A., N. Kelly, and Cicchino N. Development of the ear, hearing capabilities and laterophysic connection in the spotfin butterflyfish (chaetodon ocellatus). *Environ Biol Fish*, 95:275–290, 2012.

[85] G B West, J H Brown, and B J Enquist. A general model for the origin of allometric scaling laws in biology. *Science (New York, N.Y.)*, 276(5309):122–6, April 1997.

[86] Bogdan Wozniak and Jerzy Dera. *Light Absorption in Sea Water*. Springer New York, New York, NY, USA, 2007.

[87] Kj Wright, Dm Higgs, and Jm Leis. Ontogenetic and interspecific variation in hearing ability in marine fish larvae. *Marine Ecology Progress Series*, 424:1–13, March 2011.

[88] Hidekatsu Yamazaki, DL Mackas, and KL Denman. Coupling small-scale physical processes with biology. *The sea: Biological-Physical Interactions in the Ocean*, 12:51–112, 2002.

[89] Jeannette Yen, Petra H. Lenz, Donald V. Gassie, and Daniel K. Hartline. Mechanoreception in marine copepods: Electrophysiological studies on the first antennae. *Journal of Plankton Research*, 14:495–512, 1992.

[90] Yayoi M Yoshida, Tadamichi Morisaka, Mai Sakai, Mari Iwasaki, Ikuo Wakabayashi, Atsushi Seko, Masahiko Kasamatsu, Tomonari Akamatsu, and Shiro Kohshima. Sound variation and function in captive Commerson's dolphins (Cephalorhynchus commersonii). *Behavioural processes*, 108C:11–19, September 2014.

A List of Symbols

Symbol	Description	Units
L	Size of the organism	[m]
ϵ	Turbulent dissipation rate	[$m^2 s^{-3}$]
ρ	Density of seawater	[kg m^{-3}]
μ	Dynamic viscosity of seawater	[$kgm^{-1}s^{-1}$]
ν	Kinematic viscosity of seawater	[m^2 s^{-1}]
c	Speed of sound in sea water	[ms^{-1}]
Γ	Adiabatic index	[-]
z	Depth below the surface	[m]
g	Acceleration due to gravity	[ms^{-2}]
P	hydrostatic pressure	[Nm^{-2}]
ω	Resonance frequency	[s^{-1}]
D	Molecular diffusivity	[m^2 s^{-1}]
L_{B}	Batchelor scale	[m]
L_{K}	Kolmogorov scale	[m]
L_{I}	Integral length scale	[m]
r	Radial distance from object	[m]
U	Velocity of moving organism	[m s^{-1}]
Re	Reynolds number	[-]
L_{eye}	Axial size of eye ball	[m]
d	Photoreceptor width	[m]
C_a	Light contrast: Apparent	[-]
$C_{\mathrm{t,min}}$	Light contrast: min. threshold	[-]
C_0	Light contrast: Inherent	[-]
ρ_{ph}	Photoreceptor density	[m^{-2}]
K	Sensitivity constant of eye	[-]
I_e, I_r	Emitted, reflected sound intensity	[W/m^2]
f_c	Center frequency	[s^{-1}]
α	Light absorption in seawater	[m^{-1}]

Table 2: List of Symbols

Supplementary Information: Size Structures Sensory Hierarchy in Ocean Life

Erik A. Martens[♯],[1,2,3] Navish Wadhwa[♯],[1,4] Nis S. Jacobsen,[1,2] Christian Lindemann,[1,2] Ken H. Andersen,[1,2] and André Visser[1,2]

[1]*Centre for Ocean Life*
[2]*National Institute of Aquatic Resources, Technical University of Denmark, Charlottenlund Slot, Jægersborg Alle, DK-2920 Charlottenlund, Denmark*
[3]*Department of Biomedical Sciences, Copenhagen University, Blegdamsvej 3, 2200 Copenhagen, Denmark*[*]
[4]*Department of Physics, Technical University of Denmark, DK-2800 Kgs. Lyngby, Denmark*[†]

I. SENSING RANGE FOR VISION

The sensing range condition in the main text is given by

$$C_0 e^{-\alpha R} \geq C_{\mathrm{th,min}} + K R^2 L^{-4}. \tag{1}$$

Rescaling the sensing range, $\tilde{R} = \alpha R$ and the size, $\tilde{L} = (C_0 \alpha^2 / K)^{1/4}$ where $C := C_{\mathrm{th,min}}/C_0$, this becomes

$$e^{-\tilde{R}} \geq C + \tilde{R}^2 \tilde{L}^{-4}. \tag{2}$$

The clear-water limit corresponds to small $\tilde{R} \ll 1$, yielding

$$\tilde{R} \sim \tilde{L}^2 (1-C)^{1/2}, \tag{3}$$

and the turbid-water corresponds to large $\tilde{L}$, yielding

$$\tilde{R} \sim -\ln(C)/\alpha. \tag{4}$$

These expressions match the ones presented in the main text. Letting the two expressions for the rescaled sensing ranges (3) and (4) be similar, we arrive at the condition for the cross-over between the two regimes:

$$\tilde{L}_x^2 \sim -\ln(C)/(1-C)^{1/2}, \tag{5}$$

which in the original unscaled variables becomes $L_{\mathrm{x}}^2 \sim \alpha^{-1} K^{\frac{1}{2}} (C_0 - C_{\mathrm{th,min}})^{-\frac{1}{2}} \ln(C_0/C_{\mathrm{th,min}})$ or, to leading order,

$$L_{\mathrm{x}}^2 \sim \alpha^{-1} K^{\frac{1}{2}} (C_0 - C_{\mathrm{th,min}})^{-\frac{1}{2}}. \tag{6}$$

The clear water limit occurs for $L \ll L_x$ and the turbid water limit for $L \gg L_x$. Thus, the turbid limit is reached in the limit of large α, large $(C_0 - C_{\mathrm{th,min}})$, or small sensitivity K, respectively.

Another (rough) estimate of the minimal body size, for which vision is still marginally meaningful, could be obtained from the condition that $L \sim R$. This condition has at most two solutions, whereas the minimal solution is $L \approx [K/(C_0 - C_{\mathrm{th,min}})]^{1/2}$. A precise determination of this estimate of the smallest animal carrying an eye is, however, difficult due to the unknown scaling coefficient in this estimate and uncertainties concerning parameter values.

[*] Equal contribution.; erik.martens@sund.ku.dk
[†] Equal contribution.; nawa@fysik.dtu.dk

II. ECHOLOCATION

A. Echolocation sensing range

In the main text, we discuss that the intensity of echolocation pulses attenuates like $(2R)^{-2} e^{-2\mu R}$, where the factor 2 arises due to the double travel distance. Here, we provide in some more detail our estimates for the effects of attenuation due to geometric divergence and absorption processes in seawater.

First we discuss the effect of absorption processes on the transmission of pulses. To begin, we note that the absorption coefficient μ is frequency dependent. Each pulse is transmitted and characterized by its center (or carrier) frequency f_c, which is also the dominant frequency of the pulse spectrum. Accordingly, we may disregard all other frequencies and thus the dispersion of the transmitted pulse, leaving us with the task to find the absorption coefficient for f_c. The attenuation of sound in seawater is a complex molecular process which occurs both due to viscous absorption generated by particle motion, but also due to molecular relaxation processes by Boric acid and Magnesium sulphate. A formula for the frequency dependent absorption has been devised [1]. However, this relation is too complicated for our purposes as we desire to establish a simple asymptotic scaling relation between f_c and μ; indeed, the data is well *parameterized* by a $\mu \sim f_c^{4/3}$ (see Figure 2 below). Further, it is known that f_c depends on body size; experimental data [4] for dolphins (excluding river dolphins), allows us to heuristically deduce a scaling dependence for the absorption, $f_c \approx 370\ \mathrm{m}^{3/4}\ \mathrm{s}^{-1} \times L^{-3/4}$ (see Supplementary Text II B for details). In sum, we obtain the relation $\mu \simeq 0.0424/L$ for the absorption coefficient. Finally, since the fitted data is measured in the logarithmic decibel scale, the attenuation factor due to absorption converts to $10^{-\alpha(L)\times 2R/10}$.

Summed up, the intensity is reduced by a factor $I_r/I_e \sim R^{-2} 10^{-0.00424\times 2R/L}$. A further analysis shows that the effect of damping is in fact negligible when compared to the geometric divergence. Thus, the reduction factor simplifies to $I_r \sim L^{3\phi} L_o^2 R^{-2}$.

Center frequencies of echolocation signals have been measured for dolphins [4], shown in Figure 1. Note that the two river dolphins discussed in [4] are excluded from our analysis, since dolphins in such environments operate at different frequencies to adapt for sound transmission in non-free environments. We fitted the relation between the body mass m

and the center frequency by $f_c \approx (368.7\ \mathrm{m}^{0.26}\ \mathrm{s}^{-1}) \times m^{-0.26}$ where $m \sim \rho L^3$.

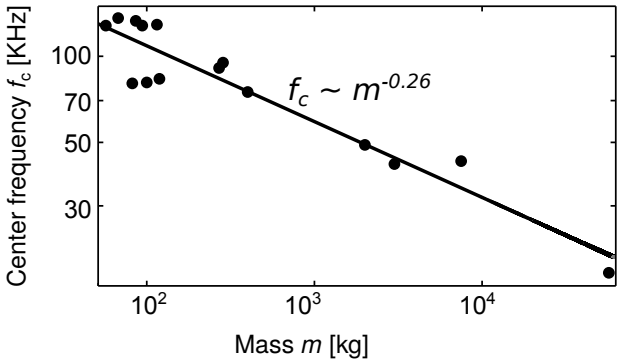

FIG. 1. Power law fit for echolocation center frequencies of dolphins. Data from [4]: f_c = (17.5, 42, 43, 75, 49, 95, 83.4, 80.4, 91, 81, 128, 136, 129, 133, 128) kHz; m = (57000, 3000, 7500, 400, 2000, 285, 119, 82, 270, 100, 94, 67.5, 115, 86, 57) kg is fitted with $f_c \approx (368.7\ \mathrm{m}^{0.26}\ \mathrm{s}^{-1}) \times m^{-0.26}$.

We note that the frequency with maximal intensity produced in the nasal sac is approximated by the Helmholtz frequency [2]:

$$f_p = \frac{c}{2\pi}\left(\frac{A}{V\ L_\mathrm{t}}\right)^{1/2} = k \times L^{-1}. \tag{7}$$

where A, V, L_t are the area, volume and length of the nasal sac. Given that m is proportional to L^3, the scaling observed in Fig. 1 appears to deviate somewhat from the theoretical estimate, which may be explained by the simplicity of the Helmholtz oscillator model.

B. Sound absorption in marine environments

The authors in [1] derive a simplified equation of the form

$$\mu = A_1 P_1 f_1 f_c^2/(f_1^2 + f_c^2) + A_2 f_2 f_c^2/(f_2^2 + f_c^2) + A_3 P_3 f_c^2 \tag{8}$$

where the center frequency f_c is measured in Hz the depth d in km. Further, they determine the following coefficients characteristic to the properties of seawater for boron and for magnesium,

$$\begin{aligned} f_1 &= 0.78 * (S/35)^{1/2} e^{T/26} \\ f_2 &= 42 e^{T/17} \\ A_1 &= 0.106 \\ A_2 &= 0.52 * (1 + T/43)(S/35) \\ A_3 &= 0.00049 \\ P_1 &= e^{(pH-8)/0.56} \\ P_2 &= e^{-z/6} \\ P_3 &= e^{-(T/27+z/17)}. \end{aligned}$$

Location	pH	S [ppt]	T [C]	z [km]
Pacific	7.7	34	4	1
Red Sea	8.2	40	22	0.2
Arctic Ocean	8.2	30	-1.5	0
Baltic Sea	7.9	8	4	0

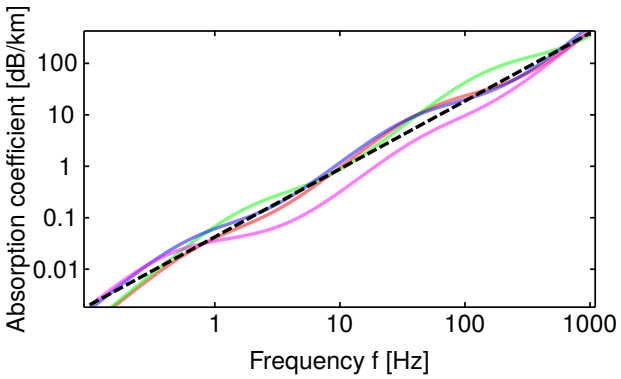

FIG. 2. Power law fit for relation between frequency and sound absorption coefficient in the ocean. **Top:** Parameter values for pH, S, T, z for Eq. 8 valid for different ocean regions. **Bottom:** Absorption rates resulting from parameters for the various regions listed in the top table. Fitting the logarithmic data linearly (dashed line) over the frequency range of interest results in the asymptotic scaling relation $\mu \approx (0.0434\ \mathrm{s}^{-1.32}\mathrm{m}^{-1}) \times f^{1.32}$.

C. Assumptions in echolocation sensing range argument

The scaling argument for the echolocation range rests on assumptions which are supported by data only in part, which we list here again for clarity:

(A1) the threshold sensitivity of the ear I_0 is independent of target size L. This approximation is supported by audiograms (behavioral and auditory brain stem responses) of odontocetes [3, 6–9],

(A2) the emitted sound intensity that an animal produces scales with size: $I_e \propto L^{3\phi}$ where $3/4 < \phi < 1$,

(A3) the carrier frequency of the sonar signal depends on size L.

Assumption (A3) is fairly well corroborated, as already discussed in section A and B. Assumption (A2) states that the scaling exponent ϕ is allowed to vary in a small range corresponding to a sublinear volume dependence of the generating organ size which; this is a fairly reasonable assumption. Taking into account the considerable scatter of the data, we recognize that the prediction compares with the data reasonably well, as is evidenced in Figure 7 in the main text. However, better data is required to further underpin assumption (A1). Indeed, within the group of whales and dolphins we find no clear size-dependent scaling for the sensitivity threshold I_0 [3]; but it would be desirable to obtain more data to solidify this assumption, as well as to identify a satisfactory physical or biological explanation for why the sensitivity is independent of body size, in contrast to other mammal groups [3, 5–8]. To be explicit, drawing the parallel between the receiving

organ and a parabolic dish, one might expect that the sensing organ has a gain factor proportional to the area of the receiving membrane, $A \propto L^2$. Accordingly, one might expect that the sensitivity scales like $I_0 \sim A^{-1} \sim L^{-2}$, which implies that the sensing range rather scales like $R \sim L^{\gamma}$ with $2.125 \leq \gamma \leq 2.5$.

[1] MA Ainslie and JG McColm. A simplified formula for viscous and chemical absorption in sea water. *The Journal of the Acoustical Society of America*, 103(June 1997):1997–1998, 1998.

[2] JL Aroyan, MA McDonald, SC Webb, JA Hildebrand, D Clark, JT Laitman, and JS Reidenberg. Acoustic models of sound production and propagation. In *Hearing by whales and ...*, number 2000. 2000.

[3] DOSITS.org. What sounds can animals hear? *Discovery of Sound in the Sea (dosits.org)*, 2014.

[4] Frants H Jensen, Alice Rocco, Rubaiyat M Mansur, Brian D Smith, Vincent M Janik, and Peter T Madsen. Clicking in shallow rivers: short-range echolocation of irrawaddy and ganges river dolphins in a shallow, acoustically complex habitat. *PloS one*, 8(4):e59284, January 2013.

[5] Ronald a. Kastelein, Paulien Bunskoek, Monique Hagedoorn, Whitlow W. L. Au, and Dick de Haan. Audiogram of a harbor porpoise (Phocoena phocoena) measured with narrow-band frequency-modulated signals. *The Journal of the Acoustical Society of America*, 112(1):334, 2002.

[6] Paul E. Nachtigall, T. Aran Mooney, Kristen a. Taylor, and Michelle M. L. Yuen. Hearing and Auditory Evoked Potential Methods Applied to Odontocete Cetaceans. *Aquatic Mammals*, 33(1):6–13, January 2007.

[7] A F Pacini, P E Nachtigall, L N Kloepper, M Linnenschmidt, A Sogorb, and S Matias. Audiogram of a formerly stranded long-finned pilot whale (Globicephala melas) measured using auditory evoked potentials. *The Journal of experimental biology*, 213:3138–3143, 2010.

[8] Aude F Pacini, Paul E Nachtigall, Christopher T Quintos, T David Schofield, Dera a Look, Gregg a Levine, and Jason P Turner. Audiogram of a stranded Blainville's beaked whale (Mesoplodon densirostris) measured using auditory evoked potentials. *The Journal of experimental biology*, 214(Pt 14):2409–15, July 2011.

[9] Jonas Teilmann, Lee A Miller, Tim Kirketerp, Ronald A Kastelein, Peter T Madsen, Bjarke K Nielsen, and Whitlow W L Au. Characteristics of echolocation signals used by a harbour porpoise (*Phocoena phocoena*) in a target detection experiment. *Aquatic Mammals*, 28:275–284, 2002.